



# Damage detection and self-healing of carbon fiber polypropylene (CFPP)/carbon nanotube (CNT) nano-composite via addressable conducting network

Sung-Jun Joo<sup>a</sup>, Myeong-Hyeon Yu<sup>a</sup>, Won Seock Kim<sup>b</sup>, Hak-Sung Kim<sup>a,c,\*</sup>

<sup>a</sup> Department of Mechanical Engineering, Hanyang University, 222 Wasngsimni-ro, Seongdong-gu, Seoul, 04763, Republic of Korea

<sup>b</sup> R&D Center, Lotte Chemical, 115 Gajeongbuk-ro, Yuseong-gu, Daejeon, Republic of Korea

<sup>c</sup> Institute of Nano Science and Technology, Hanyang University, Seoul, 04763, Republic of Korea

## ARTICLE INFO

### Keywords:

Carbon fiber polypropylene/carbon nanotube nano-composite  
Addressable conducting network  
Electrical resistance change method  
Damage monitoring  
Self-healing

## ABSTRACT

In this work, damage sensing and self-healing of carbon fiber polypropylene (CFPP)/carbon nanotube (CNT) nano-composite were performed based on addressable conducting network (ACN). To increase damage sensing resolution of CFPP/CNT nano-composite, through-thickness electrical conductivity was improved by adjusting press condition and spraying carbon nanotubes (CNT) between prepregs. From the results, electrical resistivity in thickness direction was reduced to 19.44 Ω·mm under 1.0 MPa and 1.0 wt% of CNT condition. Also, self-healing efficiency was examined with respect to the temperature and time via resistive heating of CFPP/CNT nano-composite. As a result, the optimized fabrication and self-healing condition exhibited high resolution of damage sensing with outstanding self-healing efficiency (96.83%) under fourth cycle of repeated three-point bending test.

## 1. Introduction

Carbon fiber reinforced polymer (CFRP) has received considerable attention as an innovative material due to their high strength and stiffness, light weight, resistance to fatigue/corrosion, and design flexibility [1–5]. Thus, aircraft such as Boeing 787 (Boeing Co.) and Airbus A350 (Airbus Co.) replaced more than 50% of the aircraft body with composite materials [6]. Also, a wide range of applications can be found such as aerospace, automobile, wind blade, robot, and etc.

Generally, CFRP composite is usually fabricated by stacking and curing multiples sheets of unidirectional prepregs. It has excellent mechanical properties in fiber direction. However, it has weak mechanical strength in transverse direction (matrix-rich area) that is susceptible to delamination or matrix cracking between prepregs [7,8]. Also, various severe conditions can be faced under in-service of composite, such as severe weather condition, impact damage due to hailstone or bird strike, and lightning strikes [9,10]. Therefore, structural health monitoring for damage detection is needed for assuring reliability and safety of the structures.

Nondestructive evaluation (NDE) methods such as ultrasound inspection, radiography testing, thermography, and terahertz were developed to detect damage of composites [11–16]. However, these

methods require out of service for damage inspection with labor-intensive characteristics. Moreover, most of damages are small and not visually detectable due to complexity of structure [17], resulting in fatal failure of structure due to crack propagation. Accordingly, real-time inspection system is required to detect composite damage. However, damage detection in early stage is difficult and challenging because most of micro-damages are too small to be detected [18].

Therefore, damage detection methods based on distributed smart sensors were actively developed to perform *in-situ* damage sensing with high resolution. However, damage detection methods such as piezoelectric sensor and optical fiber sensors embedded system had serious drawbacks those are high fragility, high current or voltage for operation, non-negligible weight, and high cost [19,20]. Also, insert of sensors in composite material can be a damage initiation area. Moreover, high cost of these sensors make it difficult to large-area application. Therefore, the use of nano-composite is considered as an alternative way for damage detection of composite. Nano-composite is fiber-reinforced prepregs containing functional conductive nano-materials in polymer matrix. Various nano-materials were employed, including CNT, carbon nanofibers, graphene, and other carbon-based nanomaterials [21–23]. Conductive nano-materials in matrix form conductive network in composite, enabling self-sensing ability of defects or

\* Corresponding author. Department of Mechanical Engineering, Hanyang University, 222 Wasngsimni-ro, Seongdong-gu, Seoul, 04763, Republic of Korea.  
E-mail address: [kima@hanyang.ac.kr](mailto:kima@hanyang.ac.kr) (H.-S. Kim).

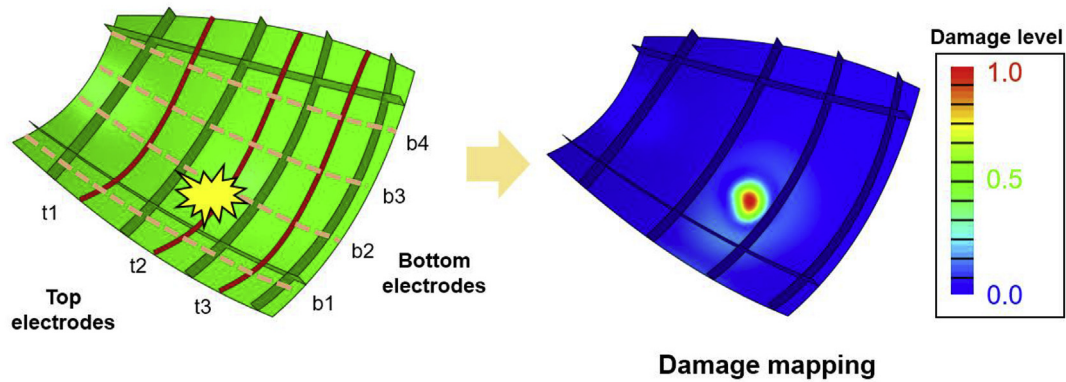


Fig. 1. Schematic illustration of addressable conducting network (ACN).

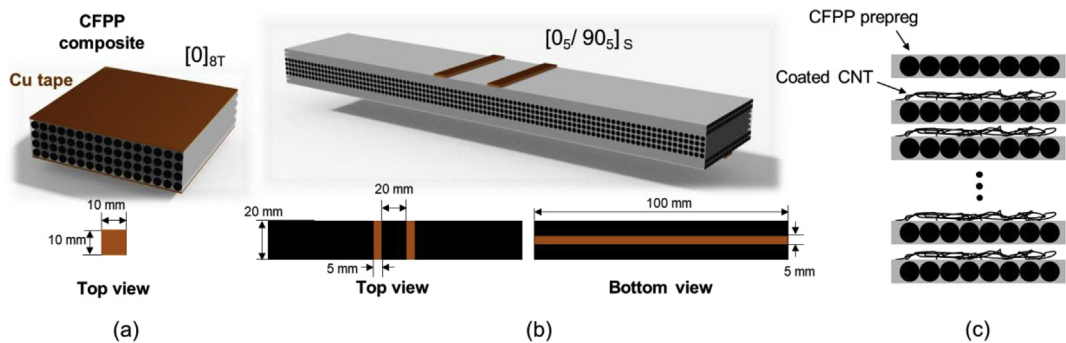


Fig. 2. Prepared samples: (a) resistivity measurement sample (panel type) and (b) self-healing sample (coupon type). (c) Schematic of stacked laminates after CNT coating process.

damages through electrical conductivity change. Among various nanomaterials, CNT is one of the promising material that is increasingly adopted for the various industrial applications due to multifunctional property. It forms electrically conductive network even at low weight concentrations, acting as distributed sensors in composite part [6,24,25]. Also, CNT improved fracture toughness significantly between laminates, facilitating multi-functional composite integrating structural and sensing capabilities [26,27].

Once nano-composite is combined with addressable conducting network (ACN) technique, it can be powerful method for damage sensing of composite. This technique is based on electrical resistance change method (ERCM), it utilizes electrically conductive network of composite itself as sensor: structural delamination or damage can be evaluated through resistance change by interruption of electric current flow. More specifically, schematic illustration of ACN is in Fig. 1, it uses multiple metallic lines on upper- and bottom-surfaces of composite. Metallic lines of each surface are parallel, and bottom- and top-electrodes are perpendicular to each other, and these lines make a grid arrangement. From the measurement of through thickness resistance change between top ( $tx$ )- and bottom ( $bx$ )-electrodes one by one (i.e.  $t1-b1$ ,  $t2-b2$  ...,  $tx-bx$ ) using pair of lines ( $tx$ ,  $by$ ), localized damage sensing can be simply evaluated by collecting resistance change of nodal points ( $x$ ,  $y$ ) [28–30]. In addition, the use of thermoplastic matrix has advantage of self-healing capability through resistive heating by supplying electrical current using same conducting lines. Therefore, the use of carbon fiber polypropylene (CFPP) composite is a good example that matrix healing reaction can be generated by melting polypropylene (PP) material through electrical heating [31–34]. This method has outstanding merits, including *in-situ* detection, no structural degradation of mechanical property, and enabling damage detection with minimization of time and cost without structural modification of composite. However, simultaneous study of damage sensing and healing behavior using CFPP composite via ACN was not deeply studied

yet.

In this work, damage monitoring and self-healing of CFPP/CNT nano-composite was investigated based on ACN. To increase damage sensing ability of composite, fabrication condition was changed such as adjusting press condition and spraying carbon nanotube (CNT) between prepregs. Self-healing test of CFPP/CNT nano-composite was conducted with various resistive heating conditions (i.e. healing temperature and time) to increase healing efficiency of CFPP/CNT nano-composite. Based on upper results, damage sensing resolution and self-healing efficiency were evaluated.

## 2. Experimental

### 2.1. Fabrication procedure of CFPP/CNT nano-composite

The composite specimens were manufactured using unidirectional CFPP prepregs (Lotte chemical) with 0.15 mm thickness by hand lay-up. Detailed specimen geometry is shown in Fig. 2(a) and (b), two different kinds of specimens were used in this work:  $[0]_{8T}$  (total 8 sheets of prepregs) for electrical conductivity measurement in thickness direction (Fig. 2(a), panel type specimen) and  $[0_s/90_s]_s$  (total 20 sheets of prepregs) for self-healing via resistive heating (Fig. 2(b), coupon type specimen). Cu-tape was additionally attached on the surface of the specimens for conducting line or pad. Then, the stacked CFPP prepregs were placed and heated to 220 °C for 10 min using hot press machine (Ocean science, Korea). Heated and pressed laminates were cooled at 1 °C/min. In order to increase electrical conductivity in thickness direction, press condition was changed from 0.1 to 1.5 MPa. Also, CNT (CM-280, Hanwha Chemical) was spread between CFPP prepregs to further improve the through-thickness electrical conductivity. Before spreading of CNT between prepregs, it was separately acid treated under 1 mol/L of  $H_2SO_4/HNO_3$  (v/v:3/1) for the good dispersion in solvent [35–38]. Then, acid treated CNT was added to ethanol and

dispersed using an ultra-sonicator (SD-200H, MUJIGAE) for 1 h. Dispersed solution was coated between preregs using spraying equipment to enhance electrical conductivity of CFPP/CNT nano-composite (Fig. 2(c)).

## 2.2. Measurement of electrical conductivity in thickness direction

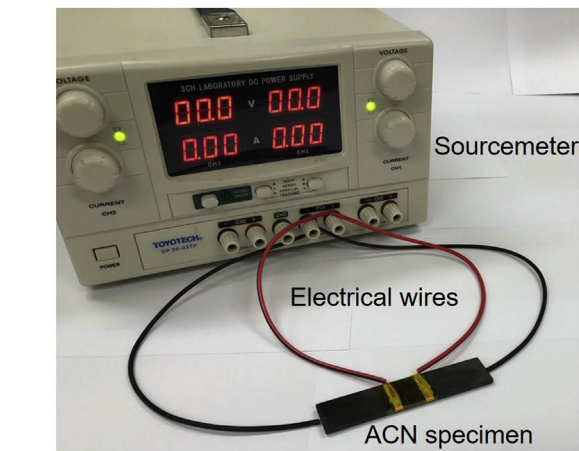
To measure the electrical conductivity in thickness direction, fabricated CFPP composite [0]<sub>ST</sub> was cut with 1 cm × 1 cm size using waterjet cutting machine (Fig. 2(a)). Two-probe method was used to measure the through thickness resistance using multimeter (2015 THD, Keithley). Meanwhile, contact resistance was measured and removed from the resistance measurements between two electrodes on the same surface with several distances and its intercept by linear approximation. Hence, the measured resistance in thickness direction by two-probe method was converted to the through-thickness resistivity ( $\rho_t$ ) by following relation [39]:

$$\rho_t = \frac{RA}{t} \quad (1)$$

where  $\rho_t$ ,  $R$ ,  $A$ , and  $t$  are through-thickness resistivity, measured resistance, area of composite (1 cm × 1 cm), and thickness of composite, respectively.  $\rho_t$  was evaluated with respect to various composite fabrication conditions as mentioned above (i.e. press condition and wt% of CNT between preregs).

## 2.3. Self-healing test via resistive heating

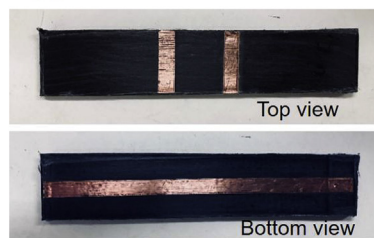
Self-healing test was performed via resistive heating of CFPP/CNT nano-composite. Fig. 3(a) shows the schematic of experimental setup for resistive heating equipment. Each conducting line was connected to the power supply (TDP-2005B, TOYOTECH) by electrical wires. In order to minimize contact resistance between electrical wire and conducting line, Ag paste was used to each contact points. Then, polyimide



(a)



(b)



(c)

Fig. 3. (a) Experiment setup for self-healing test, (b) Optical image of three-point bending test and (c) photograph of specimen.

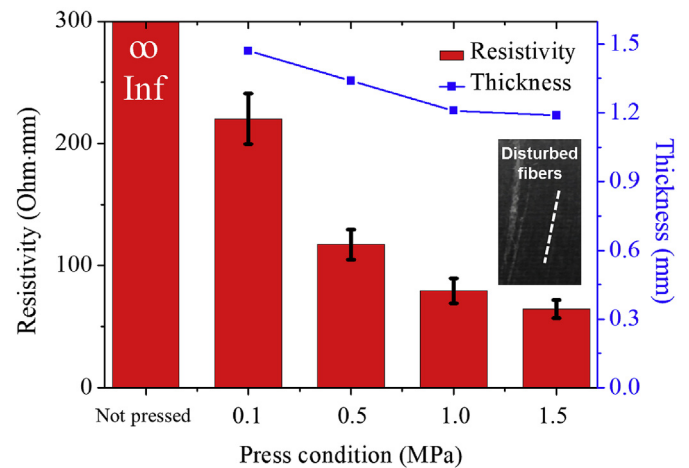


Fig. 4. Resistivity measurement result and thickness of sample with respect to press condition. Inset Fig. shows disturbed carbon fibers under 1.5 MPa condition.

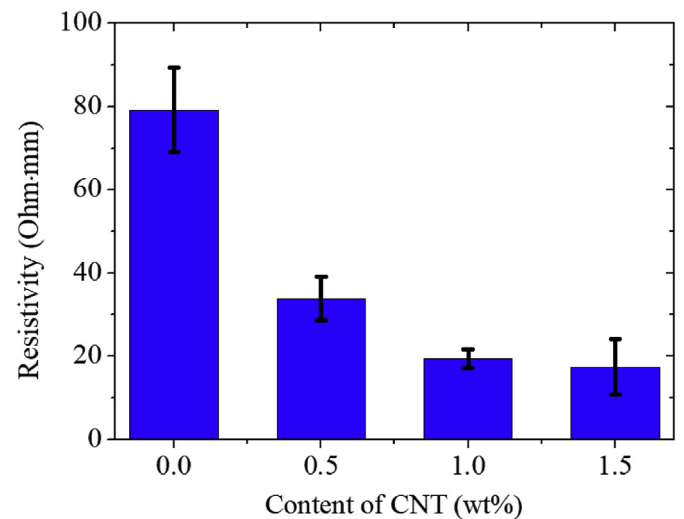


Fig. 5. Resistivity measurement result with respect to wt% of CNT.

(PI) tape was attached to the top- and bottom-of the specimen to prevent oxidation of Cu tape.

Using the above equipment, resistive heating test was conducted. Temperature of CFPP/CNT nano-composite was measured about current input from 1.0 to 1.4 A. After then, self-healing efficiency of CFPP/CNT nano-composite was assessed by repeated three-point bending test data those were performed using universal testing machine (RB 301, UNITECH-M, R&B) (Fig. 3(b)). Samples were tested at a crosshead speed of 1 mm/min to generate a sufficient time interval between individual failures. Tested specimens were self-healed via resistive heating with respect to temperature and time. This process was repeated in three times, and self-healing efficiency of CFPP/CNT nano-composite was calculated based on maximum load from three-point bending test data.

## 2.4. Characterization

Microscopic morphology with respect to the amount of CNT between preregs was observed using scanning electron microscopy (SEM, S4800, Hitachi). Damaged and self-healed CFPP/CNT nano-composite was also investigated using cross-sectional SEM. Differential scanning calorimetric (DSC, SDT Q600/DSC Q20, PERKIN ELMER) analysis was conducted to analyze melting temperature of PP. Sample

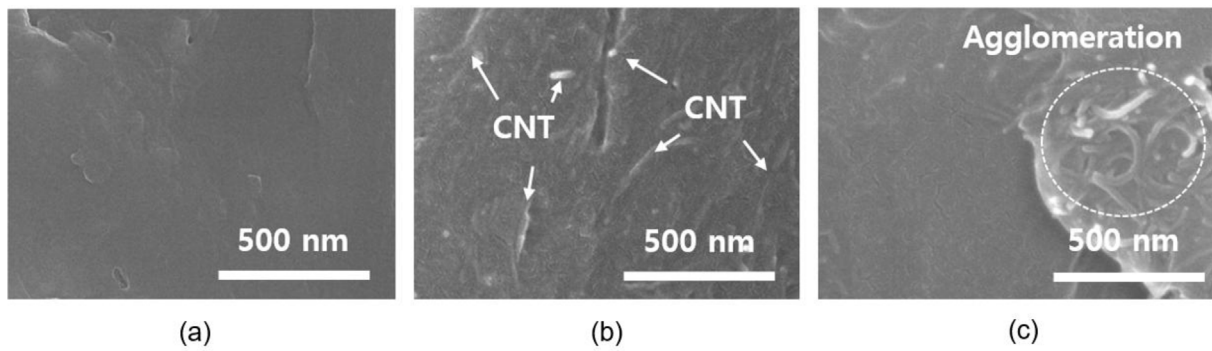


Fig. 6. Cross-sectional morphology of sample: (a) non-CNT case and (b) 1.0 wt% of CNT added case, and (c) agglomeration of CNTs in 1.5 wt% of CNT added case.

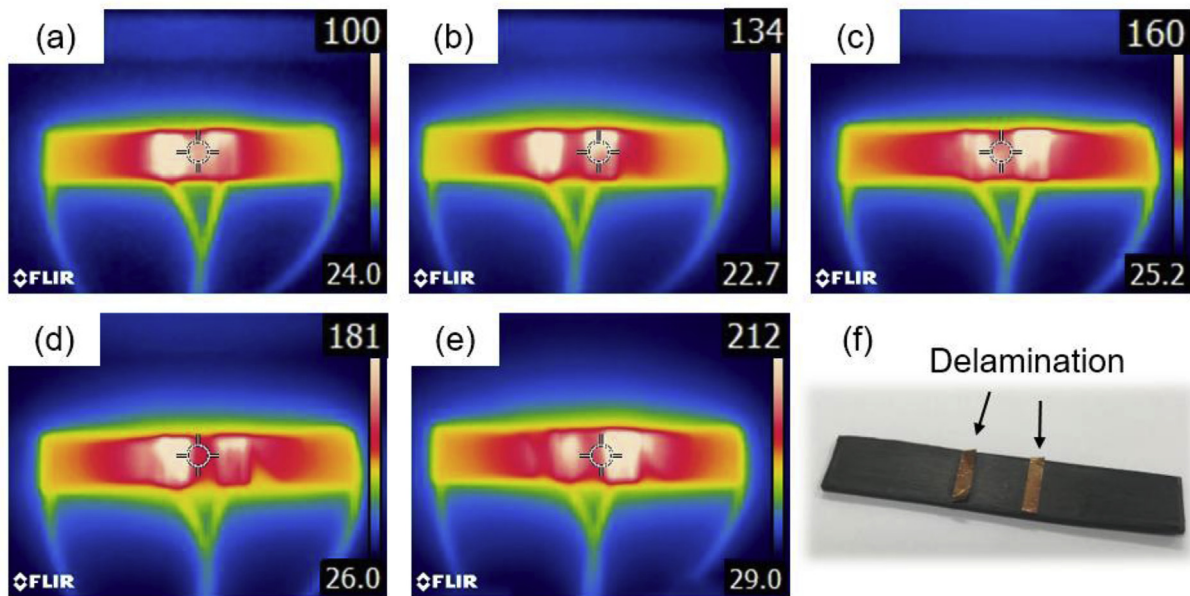


Fig. 7. Resistive heating test result: (a) 1.0, (b) 1.1, (c) 1.2, (d) 1.3, and (e) 1.4 A of current input. (f) Delamination of Cu electrode after 1.4 A (212 °C) of current input.

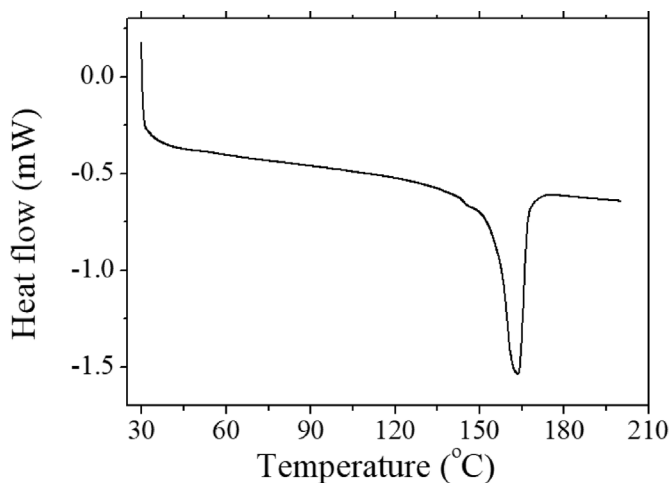


Fig. 8. DSC analysis result of CFPP prepreg.

was placed in a nitrogen atmosphere, the temperature range was from room temperature to 200 °C with 10 °C/min increase rate. Thermal conductivity in thickness direction of CFPP/CNT nano-composite was measured using a laser flash apparatus (N<sub>2</sub> gas condition, LFA 457, NETZCH) in room temperature.

### 3. Results and discussion

Firstly, fabrication condition of CFPP composite was varied to improve electrical conductivity in thickness direction. Fig. 4 shows the electrical conductivity in thickness direction with respect to pressing condition under fabrication of composite. The resistivity immediately after hand lay-up process (before fabrication of composite) was infinite, which is because carbon fibers in prepreps were not physically contact each other before the composite fabrication process. Low pressure 0.1 MPa case had high resistivity in thickness direction (220.11 Ω·mm). It is because of presence of voids or disconnection between prepreps due to low pressure during manufacturing process. This can be confirmed by the result of the thickness in Fig. 4. Thickness of sample in the case of low pressure (0.1 MPa), was higher than other cases. It means that the prepreps were not sufficiently consolidated due to the low pressure, resulting in high resistivity in thickness direction. On the contrary, the electrical conductivity was improved as the pressure was increased. Especially, 1.0 and 1.5 MPa pressure cases had relatively high electrical conductivity, 79.17 and 64.45 Ω·mm, respectively. Also, the thickness was reduced from 1.47 mm (0.1 MPa case) to 1.19 mm (1.5 MPa case) by enough to sufficient pressure [28]. Therefore, electrical conductivity in thickness direction was greatly improved with a slight decrease of thickness. However, in the case of 1.5 MPa pressure, carbon fibers were disturbed on account of high pressure (see inset Fig.

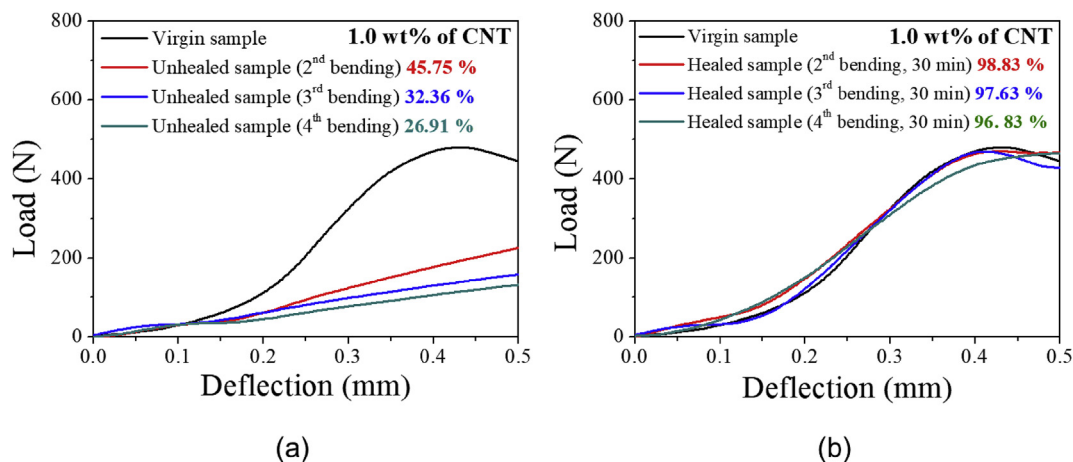


Fig. 9. Repeated three-point bending test results: (a) unhealed case, (b) 1.3 A (181 °C) heated case. All the specimens fabricated with 1.0 MPa pressing with 1.0 wt% of CNT.

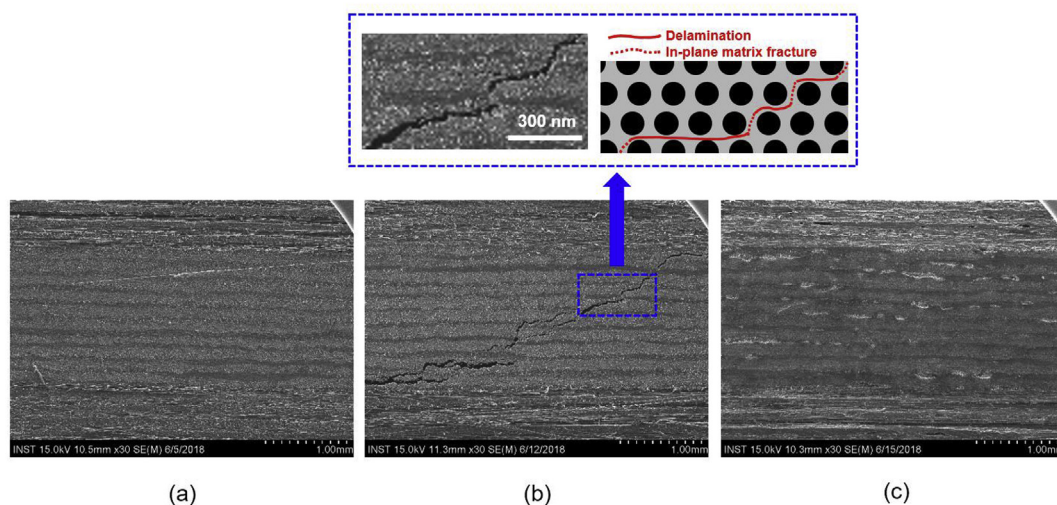


Fig. 10. Cross-sectional SEM images: (a) initial, (b) damaged, and (c) self-healed sample.

in Fig. 4). Therefore, 1.0 MPa press condition was chosen as the optimized press condition. This result can be confirmed by several reported works, several works suggested 1 MPa pressing pressure for the fabrication of PP-based composite (glass fiber/PP composite) [40,41], which is same pressure with our work. As a result, it was determined that 1 MPa pressure is needed to sufficiently impregnate the prepreps for the fabrication PP-based composite fabricated by pressing method.

To further increase the electrical conductivity in thickness direction, CNT was additionally spread between prepreps. Fig. 5 shows the electrical resistivity in thickness direction as a function of CNT amount. Notable change of electrical conductivity was observed about with increasing amount of CNT, it was greatly improved from 79.17  $\Omega$ -mm (0 wt% case) to 19.44  $\Omega$ -mm (1.5 wt% case). It is due to the addition of conductive path between carbon fibers by dispersing CNT between prepreps [42]. From SEM images in Fig. 6, CFPP composite 0.0 wt% of CNT (Fig. 6(a)) showed only PP matrix. On the contrary, 1.0 wt% CNT added cases (Fig. 6(b)) showed the well dispersed CNT in the matrix, thereby improving the electrical conductivity. However, when a large amount of CNT was added such as 1.5 wt% case, resistance was not uniform throughout specimen due to the formation of CNT agglomeration that is because of large amount of it (see agglomeration in Fig. 6(c)). Therefore, 1.5 wt% case showed a high standard deviation value in (see Fig. 5). Thus, 1.0 wt% of CNT case was considered to be the most suitable weight fraction.

Prior to the self-healing process, resistive heating test was performed. Saturation temperature of specimen was examined with respect to the current input. All the specimens were fabricated using the optimized fabrication condition (1.0 MPa pressing with 1.0 wt% CNT). Results are shown in Fig. 7; the saturated temperatures of 1.0, 1.1, 1.2, 1.3, and 1.4 A of current were 100, 134, 160, 181, and 212 °C, respectively. The saturation temperature of specimen was proportional to the current. This phenomenon is joule heating, where the heat was generated in electrical conductor such as carbon fiber and CNT because of losing its electrical energy by vibration of lattice [43]. From DSC data in Fig. 8, it was revealed that the melting point of PP matrix is around 163 °C. Thus, over 163 °C heating is required for matrix healing. However, in the 1.4 A current case (212 °C), smoke was generated from PP due to high temperature, resulting in delamination of Cu tape after heating (see delamination in Fig. 7(f)). Therefore, 1.3 A current (181 °C) heating condition was chosen for the healing of CFPP/CNT nano-composite.

Based on resistive heating data, self-healing test was performed. In this case, matrix healing time was fixed as 30 min. Also, these data were compared with no healing case. The self-healing efficiency was calculated based on the maximum load measured by three-point bending test data. Unhealed case showed low maximum load after fourth bending, only 27.53% (Fig. 9(a)). Meanwhile, 1.3 A (181 °C) heating case had relatively high self-healing efficiency (96.83%) (Fig. 9(b)), damaged

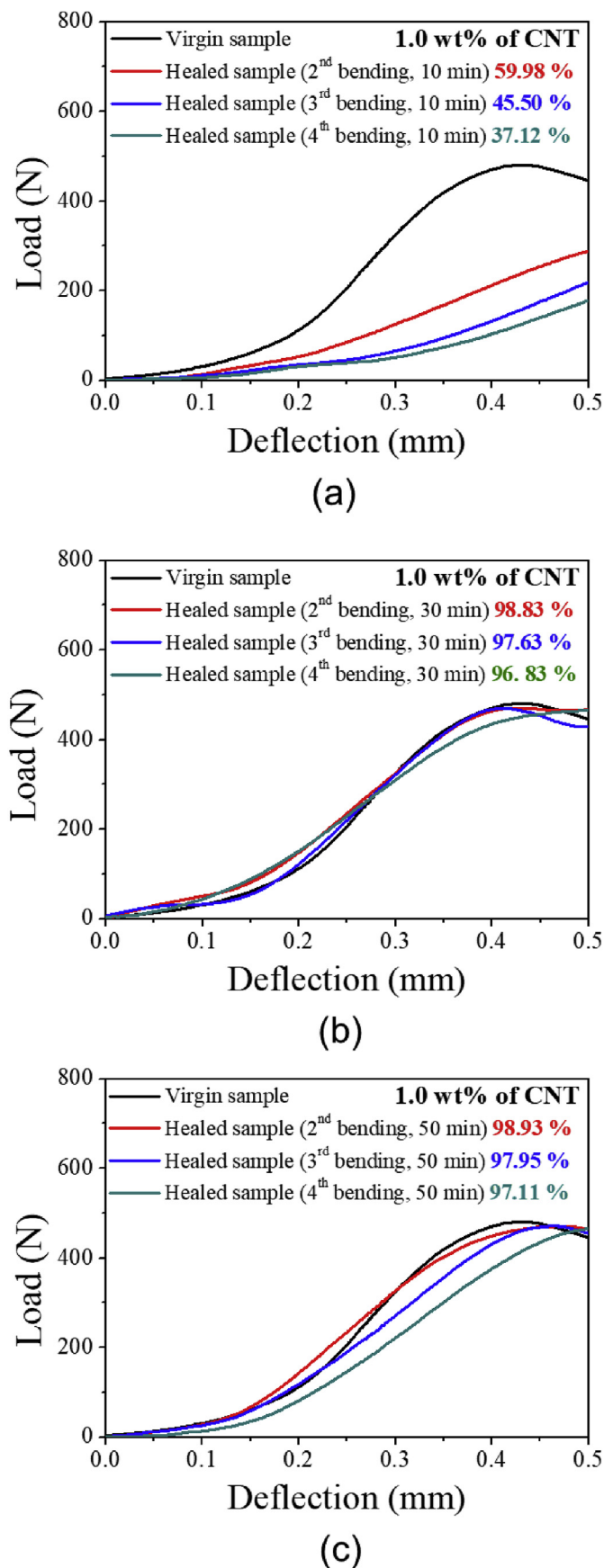


Fig. 11. Repeated three-point bending test results: (a) 10 min healing, (b) 30 min healing, and (c) 50 min healing (1.4 A, 181 °C). All the specimens fabricated with 1.0 MPa pressing with 1.0 wt% of CNT.

matrix was melt and healed under resistive heating process; delamination in composite was completely eliminated. It can be seen in cross-sectional SEM images in Fig. 10. Initial state of sample showed well-consolidated prepregs each other (Fig. 10(a)). After bending process, there was generation of crack that is inclined at 45° (Fig. 10(b)). Fig. 10(c) shows the high resolution image and schematic of damaged sample, generated crack is combination of delamination between prepregs and in-plane matrix fracture between carbon fibers. Since all the crack is matrix cracking, it can be completely healed through resistive heating process. Therefore, it can be clearly seen that all of the matrix crack was disappeared after the self-healing process as shown healed morphology in Fig. 10(c).

Also, self-healing test was performed as a function of healing time (Fig. 11). The short-healing time case (10 min healing) showed low healing efficiency, it showed only 37.12% after fourth bending test (Fig. 11(a)). From the result, it was found that 10 min healing is too short time for enough healing of damaged matrix. In other words, self-healing of damaged matrix from three-point bending test need a certain amount of time for elimination of matrix crack. Therefore, longer healing time was adopted for matrix healing. In the case of 50 min healing, it showed similar healing efficiency after fourth bending, which had similar with 30 min healing case (97.11%) (Fig. 11(c)). As a result, 181 °C temperature and 30 min healing condition was the best condition for matrix healing of CFPP/CNT nano-composite.

Based on the above results, damage sensing resolution and self-healing efficiency tests according to the composite manufacturing condition was performed. Two different coupon type specimens were used (Fig. 2(b)): 1.0 MPa press condition 0.0 wt% of CNT and 1.0 MPa press condition with 1.0 wt% of CNT. For the definition of damage sensing resolution, resistance change rate was defined as follows:

$$\Delta R = \frac{R_f - R_i}{R_i} \quad (2)$$

where  $\Delta R$ ,  $R_i$ , and  $R_f$  are resistance change rate, initial resistance (before bending test), and measured resistance after three-point bending test (or after healing process), respectively. Fig. 12(a) shows the through-thickness resistance change rate during repeated bending induced damaging and self-healing process. All the  $\Delta R$  values in thickness direction was performed at stress-free state (load = 0) after loading process. 1.0 MPa press condition 0.0 wt% of CNT case showed relatively low resistance change rate after damaging due to the high electrical resistivity in thickness direction, which means low resolution of damage detection. The resistance change rate was about 3.7%. On the contrary, 1.0 MPa press condition with 1.0 wt% of CNT case showed high degree of resistance change rate after damaging of composite, which is 4.9 times high than that of 0.0 wt% of CNT case (18.1%). From the results, it was confirmed that the damage sensing resolution is highly influenced by electrical conductivity in thickness direction [23]. These damaged specimens were self-healed via optimized resistive heating condition as found above (181 °C, 30 min). After healing, through-thickness resistance was measured again. In the graph, cycle number 0 means initial state, and odd and even numbers are after damaging and healing process, respectively (see horizontal axis in Fig. 12(a)). In the case of 1.0 wt% of CNT, it was confirmed that the rate of change of resistance after healing returned to almost zero, which indicates that the damaged matrix was completely healed. Meanwhile, in the case of 0.0 wt% of CNT, there was some residual resistance after the healing process because it was not fully healed. After then, under the repetitive damaging and healing process, 1.0 wt% of CNT case showed that the rate of resistance change was similar at each time of damaging, and resistance change rate was slightly increased but almost zero after healing process. Also, it showed high degree of healing efficiency after fourth bending, 96.83% (see Fig. 12(c)). Therefore, 1.0 wt % of CNT had stable and high resolution of damage sensing (Fig. 12(a)) as well as high healing efficiency (Fig. 12(c)). On the other hand, in the case of 0.0 wt% of CNT, the resistance change after damaging was

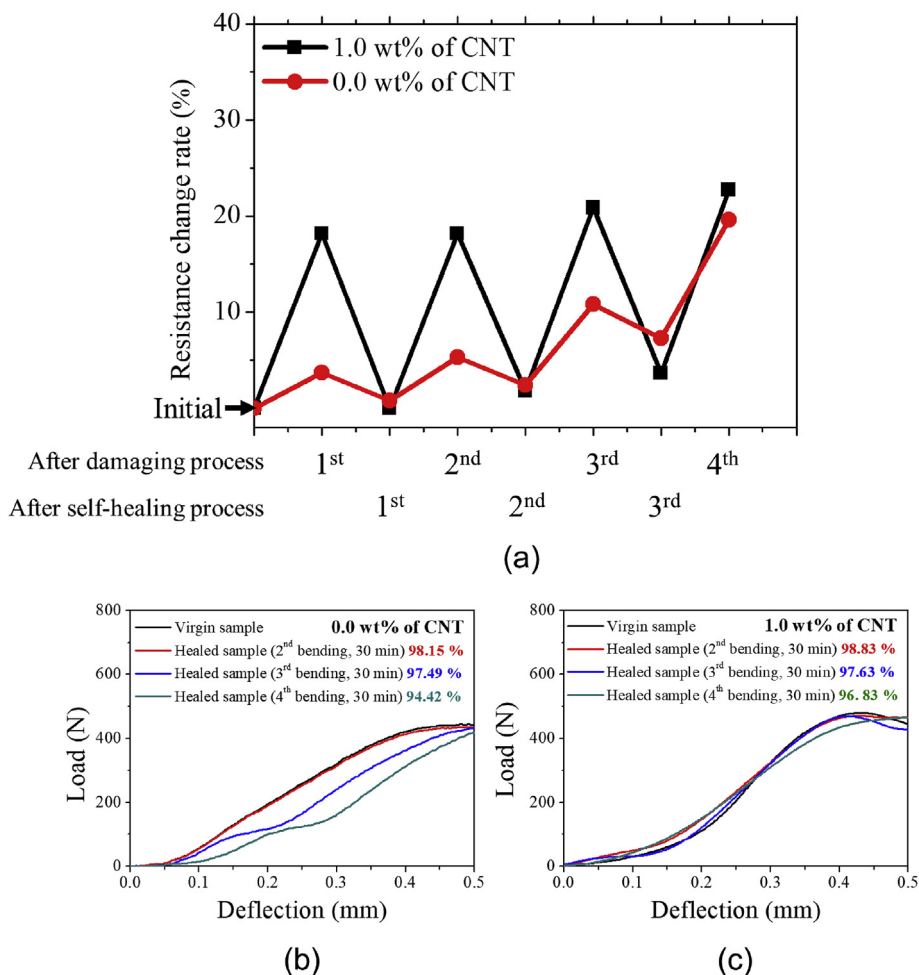


Fig. 12. (a) Through-thickness resistance change rate under the repeated damaging and self-healing process. Self-healing test result: (b) without CNT and (c) 1 wt% of CNT case.

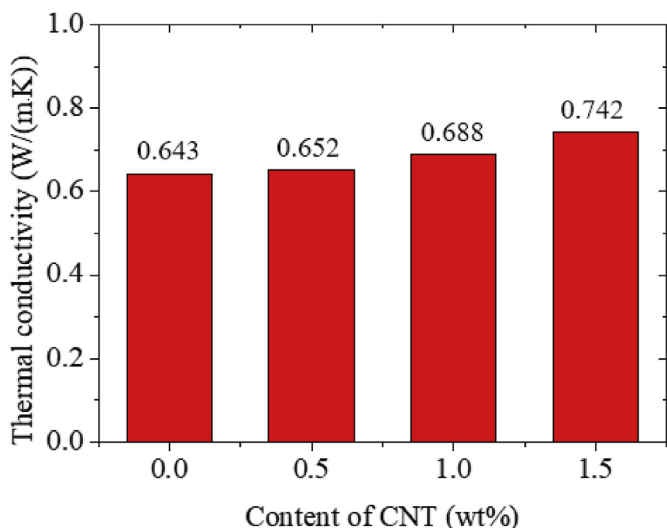


Fig. 13. Thermal conductivity measurement result with respect to wt% of CNT.

relatively low, about 4%. Furthermore, residual resistance after healing process was increased as the cycle number was increased, which is because incomplete matrix healing. Fig. 12(b) shows a consistent result that 0.0 wt% of CNT case had slightly low healing efficiency (94.42%) after fourth bending of three-point bending test. These results can be analyzed from the thermal conductivity measurement results. As shown

in Fig. 13, overall thermal conductivity in thickness direction was improved with increasing wt % of CNT. Spreading CNT between prepregs not only enhance thermal conductivity at inter-ply area, but also improved overall thermal conductivity of composite. Hence, matrix cracks were efficiently healed about CNT added case by spreading heat more evenly.

From above results, it can be explained as Fig. 14; CNT in CFPP/CNT nano-composite not only acts as electrical conductor between carbon fibers, but also spreads the heat more evenly during the healing process, resulting in high healing efficiency. Therefore, damage sensing resolution and matrix healing efficiency was greatly improved.

#### 4. Conclusion

This work demonstrates the damage mapping and self-healing of CFPP/CNT nano-composite based on ACN. To improve electrical conductivity in thickness direction, pressing condition was adjusted and CNT was spread between prepregs. From the optimized press condition, prepregs were fully impregnated with sufficient pressure. Also, CNT acts as electrical conductors between carbon fibers, resulting in increase of electrical conductivity (19.44 Ω·mm). Self-healing test was conducted via resistive heating, healing condition was varied by controlling temperature and time. From the results, 1.3 A (181 °C) with 30 min healing showed high self-healing efficiency 96.83% after fourth three-point bending test. Former technique was applied to the coupon type CFPP/CNT nano-composite specimen, which successfully exhibited high resolution of damage sensing resolution (18.1% resistance change

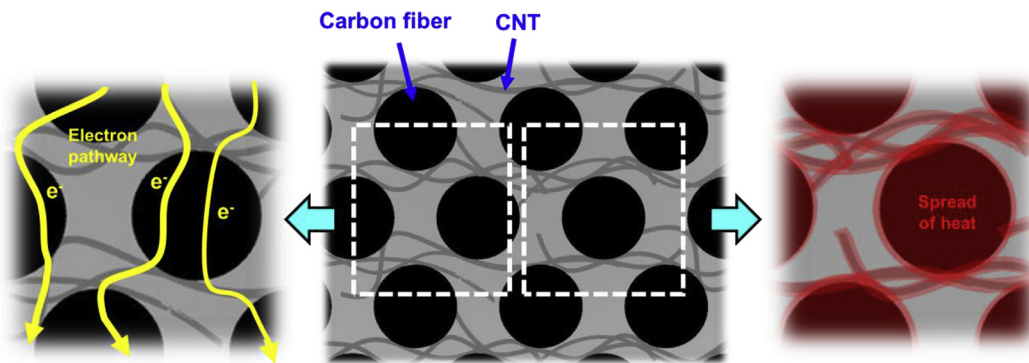


Fig. 14. A schematic illustration of mechanisms for improving damage resolution and self-healing efficiency of CNT in CF/PP composite.

rate after 0.5 mm bending) with outstanding healing efficiency (96.83% after fourth bending).

### Acknowledgements

This work was supported by the Industrial Strategic technology development program (10076562, Development of fiber reinforced thermoplastic nano-composite via fiber bundle spreading for high quality resin impregnation process and its application to the underbody shield component for protecting battery pack of an electric-vehicle) funded by the Ministry of Trade, Industry and Energy (MI, Korea). This research was supported by the National Research Foundation of Korea (NRF) funded by the Ministry of Education (2012R1A6A1029029). This research was also supported by a National Research Foundation of Korea (NRF), funded by the Korean Government (MEST) (2013M2A2A9043280) and the Ministry of Education (2015R1D1A1A09058418).

### References

- [1] K. Senthilnathan, C.P. Hiremath, N. Naik, A. Guha, A. Tewari, Microstructural damage dependent stiffness prediction of unidirectional CFRP composite under cyclic loading, *Compos. Appl. Sci. Manuf.* 100 (2017) 118–127.
- [2] A.S. Lim, Z.R. Melrose, E.T. Thostenson, T.-W. Chou, Damage sensing of adhesively-bonded hybrid composite/steel joints using carbon nanotubes, *Compos. Sci. Technol.* 71 (9) (2011) 1183–1189.
- [3] C. Wang, K. Cheng, R. Rakowski, D. Greenwood, J. Wale, Comparative studies on the effect of pilot drillings with application to high-speed drilling of carbon fibre reinforced plastic (CFRP) composites, *Int. J. Adv. Manuf. Technol.* 89 (9–12) (2017) 3243–3255.
- [4] J. Park, D. Kwon, P. Shin, J. Kim, K. DeVries, New Sensing Method of Dispersion and Damage Detection of Carbon Fiber/polypropylene-polyamide Composites via Two-dimensional Electrical Resistance Mapping, Behavior and Mechanics of Multifunctional Materials and Composites 2017, International Society for Optics and Photonics, 2017101650M.
- [5] M. Jin, B. Jin, X. Xu, X. Li, T. Wang, J. Zhang, Effects of ultrahigh molecular weight polyethylene and mould temperature on morphological evolution of isotactic polypropylene at micro-injection moulding condition, *Polym. Test.* 46 (2015) 41–49.
- [6] L. Vertuccio, L. Guadagno, G. Spinelli, P. Lamberti, M. Zarelli, S. Russo, G. Iannuzzo, Smart coatings of epoxy based CNTs designed to meet practical expectations in aeronautics, *Compos. B Eng.* 147 (2018) 42–46.
- [7] R.B. Ladani, S. Wu, A.J. Kinloch, K. Ghorbani, A.P. Mouritz, C.H. Wang, Enhancing fatigue resistance and damage characterisation in adhesively-bonded composite joints by carbon nanofibres, *Compos. Sci. Technol.* 149 (Supplement C) (2017) 116–126.
- [8] M. Fotouhi, S. Sadeghi, M. Jalalvand, M. Ahmadi, Analysis of the damage mechanisms in mixed-mode delamination of laminated composites using acoustic emission data clustering, *J. Thermoplast. Compos. Mater.* 30 (3) (2017) 318–340.
- [9] D. Kreculj, B. Rašuo, Review of impact damages modelling in laminated composite aircraft structures, *Teh. Vjesn.* 20 (3) (2013) 485–495.
- [10] N. Petrov, A. Haddad, H. Griffiths, R. Waters, Lightning strikes to aircraft radome: electric field shielding simulation, gas discharges and their applications, GD 2008. 17th International Conference on, IEEE, 2008, 2008, pp. 513–516.
- [11] C.-H. Ryu, S.-H. Park, D.-H. Kim, K.-Y. Jhang, H.-S. Kim, Nondestructive evaluation of hidden multi-delamination in a glass-fiber-reinforced plastic composite using terahertz spectroscopy, *Compos. Struct.* 156 (2016) 338–347.
- [12] D.-H. Han, L.-H. Kang, Nondestructive evaluation of GFRP composite including multi-delamination using THz spectroscopy and imaging, *Compos. Struct.* 185 (Supplement C) (2018) 161–175.
- [13] K. Zheng, Y. Yao, Automatic defect detection based on segmentation of pulsed thermographic images, *Chemometr. Intell. Lab. Syst.* 162 (Supplement C) (2017) 35–43.
- [14] K. Chatterjee, S. Tuli, S.G. Pickering, D.P. Almond, A comparison of the pulsed, lock-in and frequency modulated thermography nondestructive evaluation techniques, *NDT E Int.* 44 (7) (2011) 655–667.
- [15] M. Kaufmann, D. Zenkert, C. Mattei, Cost optimization of composite aircraft structures including variable laminate qualities, *Compos. Sci. Technol.* 68 (13) (2008) 2748–2754.
- [16] S. Park, H.-H. Shin, C.-B. Yun, Wireless impedance sensor nodes for functions of structural damage identification and sensor self-diagnosis, *Smart Mater. Struct.* 18 (5) (2009) 055001.
- [17] U. Polimeno, M. Meo, Detecting barely visible impact damage detection on aircraft composites structures, *Compos. Struct.* 91 (4) (2009) 398–402.
- [18] L. Vertuccio, V. Vittoria, L. Guadagno, F. De Santis, Strain and damage monitoring in carbon-nanotube-based composite under cyclic strain, *Compos. Appl. Sci. Manuf.* 71 (Supplement C) (2015) 9–16.
- [19] D.C. Lee, J.J. Lee, S.J. Yun, The mechanical characteristics of smart composite structures with embedded optical fiber sensors, *Compos. Struct.* 32 (1) (1995) 39–50.
- [20] D.C. Lee, J.J. Lee, Effect of embedded optical fiber sensors on transverse crack spacing of smart composite structures, *Compos. Struct.* 32 (1) (1995) 51–58.
- [21] L. Guadagno, C. Naddeo, M. Raimondo, G. Barra, L. Vertuccio, S. Russo, K. Lafdi, V. Tucci, G. Spinelli, P. Lamberti, Influence of carbon nanoparticles/epoxy matrix interaction on mechanical, electrical and transport properties of structural advanced materials, *Nanotechnology* 28 (9) (2017) 094001.
- [22] X. Du, H. Zhou, W. Sun, H.-Y. Liu, G. Zhou, H. Zhou, Y.-W. Mai, Graphene/epoxy interleaves for delamination toughening and monitoring of crack damage in carbon fibre/epoxy composite laminates, *Compos. Sci. Technol.* 140 (2017) 123–133.
- [23] C. Viets, S. Kaysser, K. Schulte, Damage mapping of GFRP via electrical resistance measurements using nanocomposite epoxy matrix systems, *Compos. B Eng.* 65 (2014) 80–88.
- [24] G. Spinelli, P. Lamberti, V. Tucci, L. Vertuccio, L. Guadagno, Experimental and theoretical study on piezoresistive properties of a structural resin reinforced with carbon nanotubes for strain sensing and damage monitoring, *Compos. B Eng.* 145 (2018) 90–99.
- [25] L. Vertuccio, L. Guadagno, G. Spinelli, P. Lamberti, V. Tucci, S. Russo, Piezoresistive properties of resin reinforced with carbon nanotubes for health-monitoring of aircraft primary structures, *Compos. B Eng.* 107 (2016) 192–202.
- [26] H. Zhang, Y. Liu, M. Kuwata, E. Bilotti, T. Peijs, Improved fracture toughness and integrated damage sensing capability by spray coated CNTs on carbon fibre prepreg, *Compos. Appl. Sci. Manuf.* 70 (2015) 102–110.
- [27] S.C. Joshi, V. Dikshit, Enhancing interlaminar fracture characteristics of woven CFRP prepreg composites through CNT dispersion, *J. Compos. Mater.* 46 (6) (2012) 665–675.
- [28] K. Takahashi, J.S. Park, H.T. Hahn, An addressable conducting network for automatic structural health management of composite structures, *Smart Mater. Struct.* 19 (10) (2010) 105023.
- [29] K. Takahashi, H.T. Hahn, Towards practical application of electrical resistance change measurement for damage monitoring using an addressable conducting network, *Struct. Health Monit.* 11 (3) (2012) 367–377.
- [30] K. Takahashi, H.T. Hahn, Investigation of temperature dependency of electrical resistance changes for structural management of graphite/polymer composite, *J. Compos. Mater.* 45 (25) (2011) 2603–2611.
- [31] Y. Heo, H.A. Sodano, Thermally responsive self-healing composites with continuous carbon fiber reinforcement, *Compos. Sci. Technol.* 118 (2015) 244–250.
- [32] N. Kwok, H.T. Hahn, Resistance heating for self-healing composites, *J. Compos. Mater.* 41 (13) (2007) 1635–1654.
- [33] J. Park, K. Takahashi, Z. Guo, Y. Wang, E. Bolanos, C. Schaffner, E. Murphy, F. Wudl, H. Hahn, A self-healing composite using a thermally remendable polymer, *J. Compos. Mater.* 42 (26) (2008) 2869–2881.
- [34] J.S. Park, H.S. Kim, H.T. Hahn, Healing behavior of a matrix crack on a carbon fiber/mendomer composite, *Compos. Sci. Technol.* 69 (7) (2009) 1082–1087.
- [35] S. Rahmam, N. Mohamed, S. Sufian, Effect of acid treatment on the multiwalled

- carbon nanotubes, *Mater. Res. Innovat.* 18 (sup6) (2014) S6-196-S6-199.
- [36] H. Misak, R. Asmatulu, M. O'Malley, E. Jurak, S. Mall, Functionalization of carbon nanotube yarn by acid treatment, *Int. J. Smart Nano Mater.* 5 (1) (2014) 34–43.
- [37] F.V. Ferreira, W. Francisco, B.R. Menezes, F.S. Brito, A.S. Coutinho, L.S. Cividanes, A.R. Coutinho, G.P. Thim, Correlation of surface treatment, dispersion and mechanical properties of HDPE/CNT nanocomposites, *Appl. Surf. Sci.* 389 (2016) 921–929.
- [38] S.-T. Kang, J.-Y. Seo, S.-H. Park, The characteristics of CNT/cement composites with acid-treated MWCNTs, *Adv. Mater. Sci. Eng.* 2015 (2015).
- [39] T. Augustin, D. Grunert, H.H. Langner, V. Haverkamp, B. Fiedler, Online monitoring of surface cracks and delaminations in carbon fiber/epoxy composites using silver nanoparticle based ink, *Adv. Manuf. Polym. Compos. Sci.* 3 (3) (2017) 110–119.
- [40] I.-G. Lee, D.-H. Kim, K.-H. Jung, H.-J. Kim, H.-S. Kim, Effect of the cooling rate on the mechanical properties of glass fiber reinforced thermoplastic composites, *Compos. Struct.* 177 (2017) 28–37.
- [41] K.-H. Jung, D.-H. Kim, H.-J. Kim, S.-H. Park, K.-Y. Jhang, H.-S. Kim, Finite element analysis of a low-velocity impact test for glass fiber-reinforced polypropylene composites considering mixed-mode interlaminar fracture toughness, *Compos. Struct.* 160 (2017) 446–456.
- [42] W. Li, D. He, Z. Dang, J. Bai, In situ damage sensing in the glass fabric reinforced epoxy composites containing CNT–Al<sub>2</sub>O<sub>3</sub> hybrids, *Compos. Sci. Technol.* 99 (2014) 8–14.
- [43] T. Ragab, C. Basaran, Joule heating in single-walled carbon nanotubes, *J. Appl. Phys.* 106 (6) (2009) 063705.